Metabolic resistance of the tiger mosquito to pyrethroid insecticides in La Réunion Island likely results from local adaptation

Tiphaine Bacot[1†], Jean-Marc Bonneville[1†], Vincent Lacroix[2], Pascal Oberbach[2], Thierry Gaude[1], Louis Nadalin[1] Frederic Laporte[1], Nausicaa Habchi-Hanriot[3], Guillaume Dupuy[3], Cyrille Czeher[3], Michael C Fontaine[4,5], Frederic Boyer[1] and Jean-Philippe David[1*]

1 Laboratoire d'Ecologie Alpine (LECA, UMR 5553), Université Grenoble-Alpes (UGA), Université Savoie Mont-Blanc (USMB), CNRS, Grenoble, France. **2** Laboratoire de Biométrie et Biologie Evolutive (LBBE, UMR 5558), CNRS, INRIA Erable, Université de Lyon, Université Lyon 1, Villeurbanne, France. **3** Agence Régional de Santé de La Réunion (ARS), Direction de la Veille et de la Sécurité Sanitaires & Santé et Milieux de vie, Service de Lutte Antivectorielle, Saint-Clotilde, France. **4** Maladies Infectieuses et Vecteurs : Ecologie, Génétique et Contrôle (MIVEGEC, UMR 5290), Université de Montpellier (UM), CNRS, IRD, Montpellier, France. **5** Groningen Institute for Evolutionary Life Sciences (GELIFES), University of Groningen, Groningen, Netherlands. **†** Equal contribution.

* jean-philippe.david@univ-grenoble-alpes.fr

Abstract

The resistance of mosquitoes to insecticides is a valuable model system for studying the genetic bases of xenobiotic adaptation in insects. The spread of the Asian tiger mosquito *Aedes albopictus* combined to the massive use of pyrethroid insecticides to limit arbovirus transmission resulted in the rise of resistance in various continents. Here, we investigated the genetic mechanisms underlying the recent adaptation of this mosquito to deltamethrin in La Réunion island. Bioassays confirmed the presence of resistance alleles in field populations. The resistance phenotype was further enhanced in the laboratory following a few generations of controlled selection. Combining whole genome Pool-seq and RNA-seq revealed no evidence of target-site resistance mutations but the over-expression and variant selection of detoxification enzymes associated with pyrethroid metabolism including cytochrome P450s, transferases and ABC-transporters. Among over-expressed detoxification genes, only one was linked to a gene duplication while polymorphism data suggest most of them being trans-regulated. Genome-wide selection signatures revealed a 9 Mb inverted superlocus responding to insecticide selection whose phenotypical importance remains uncertain. Altogether, this study indicates that the multigenic metabolic resistance phenotype observed in this insular territory mainly results from local adaptation. From an applied perspective, this study provides a set of markers to track pyrethroid resistance in the tiger mosquito in the South-West Indian Ocean. As this region is subjected to

recurrent arbovirus outbreaks, the additive resistance phenotype that may arise from the introduction of *Kdr* mutations from other territories also calls for improving resistance surveillance at the regional scale.

Author summary

While novel vector control strategies are being developed, chemical insecticides remain widely used to control mosquitoes transmitting human diseases such as the Asian tiger mosquito. However, the recurrent use of insecticides resulted in the emergence of resistance which can ultimately affect vector control efficacy. Here, we investigate the genetic bases underlying the resistance of the Asian tiger mosquito to the pyrethroid insecticide deltamethrin in La Réunion island. By combining two complementary genomic approaches, we showed that resistance is mainly caused by an increased insecticide detoxification while classical 'Knock down resistance' mutations affecting the target of the insecticide were not detected. We also showed that resistance is underlain by multiple genetic changes spread across the genome, supporting the local selection of resistance rather than the introduction of resistance alleles. Furthermore, we identified a large inverted supergene responding to insecticide selection. This study provides valuable insights into the genetic bases of insecticide resistance, enabling the implementation of molecular makers to improve the tracking of insecticide resistance in this major mosquito vector across the Indian Ocean.

Introduction

Natural populations experience a variety of human-driven selective pressures, leading to their adaptation through the expression of complex phenotypes (1). Understanding the genetic mechanisms allowing them to adapt to such rapid environmental changes provides key knowledge for populations management (2–4). The evolution of insecticide resistance is a good example of how natural selection can mediate the rapid adaptation of natural populations to anthropogenic pressures as it occurs in a large number of insects (5,6). Beyond understanding the adaptative mechanisms, identifying resistance alleles also contributes to improving management strategies (7–9). However, the frequent co-occurrence of multiple resistance mechanisms and the diversity of genetic events underlying resistant phenotypes often makes the characterization of resistance alleles challenging (5,10).

Among insect vectors, *Aedes* mosquitoes pose a significant threat to public health because they transmit major arboviral diseases (11,12). Among them, the invasive Asian tiger mosquito *Aedes albopictus* is of particular importance because its spread contributed to the worldwide re-emergence

66 of arboviruses such as dengue and chikungunya (13). Although significant research efforts are
67 dedicated to develop vaccines targeting these arboviruses (14–16), outbreak prevention still massively
68 relies on insecticide-based vector control (17). Pyrethroid insecticides such as deltamethrin are the
69 most-used insecticides against Aedes mosquitoes (18). However, the adaptation of mosquitoes to such
70 insecticides can ultimately reduce the efficacy of vector control preventive actions (19–22).

71 Pyrethroids disrupt nerve function by altering the opening kinetics of the voltage-gated sodium
72 channel (VGSC gene: 23,24). Pyrethroid resistance can be the consequence of point mutations
73 affecting the VGSC gene, known as Knock-down resistance (*Kdr*) mutations (target-site resistance); a
74 decreased insecticide penetration mediated by cuticle modification (cuticle resistance); and
75 biodegradation of the insecticide through complex detoxification pathways (metabolic resistance: 10).
76 *Kdr* mutations typically affect a few conserved amino-acid positions in the VGSC protein and are fairly
77 well characterized in *Aedes* mosquitoes (25–28). Conversely, the genetic bases of insecticide
78 detoxification are far less understood. Indeed, the diversity and redundancy of genes underlying
79 xenobiotic detoxification pathways often lead to various multigenic adaptive trajectories depending on
80 the local context (5,10,17,23). In insects, pyrethroid metabolism typically includes an initial phase
81 involving hydroxylation by cytochrome P450s and sometimes ester-bond hydrolysis by
82 carboxylesterases, followed by the conjugation of hydrophilic groups by glutathione S-transferases
83 (GSTs) and UDP-glycosyltransferases (UDPGTs), and the excretion of the insecticide itself or its
84 metabolites by ABC-transporters (29–31). Molecular changes underlying metabolic resistance to
85 pyrethroids frequently include the over-expression of detoxification enzymes and transporters
86 mediated by cis- or trans-regulation or by gene duplication although the selection of
87 enzyme/transporter variants showing an enhanced activity toward the insecticide has also been
88 described (6,32–35).

89 The recent spread of *Ae. albopictus* to all continents and its ecological shift to more urbanized areas
90 (12) led to its increased exposure to pyrethroid insecticides and ultimately to the selection of
91 resistance. Pyrethroid resistance was first reported in South-East Asia more than a decade ago (36–39)
92 followed by other Asian regions (40–42). In these regions the resistance phenotype was often related
93 to the presence of various *Kdr* mutation haplotypes (40,43,44), although metabolic resistance was also
94 detected (45–47). Resistance was then detected in Europe following the introduction of *Kdr* mutations
95 from Asia (48–50). Resistance was also detected in Africa in association with *Kdr* mutations and
96 increased detoxification though the underlying resistance alleles were not characterized (51–53).

97 In the Indian Ocean, *Ae. albopictus* was likely imported from Asia in La Réunion island during the 17th
98 and the 18th centuries though other introductions likely occurred later (54). This mosquito was
99 associated to the chikungunya outbreak that occurred in 2005-2006 (55,56) and is the main vector of

100 recurrent dengue/chikungunya outbreaks since then (57). In La Réunion island, the recurrent use of
101 deltamethrin for vector control since 2006 ultimately resulted in the emergence of resistance as
102 detected by public health authorities in 2017 (58). However, the mechanisms underlying the resistance
103 phenotype have not been thoroughly investigated since then. A single heterozygote for the V1016G
104 *Kdr* mutation was observed from mosquitoes collected in La Réunion in 2016 as part of a worldwide
105 *Kdr* screening study (59). However, the circulation of *Kdr* mutation in the island or neighbouring
106 territories was not confirmed after this observation.

107 In this context, the present work aims at deciphering the genetic bases of the deltamethrin resistance
108 phenotype observed in *Ae. albopictus* populations in La Réunion island. This was achieved by adopting
109 an experimental design combining field populations and field-derived lines enriched or not for
110 resistance alleles by controlled selection. At the molecular level, an integrated genomic approach
111 combining RNA-seq and whole genome Pool-seq was applied to pinpoint resistance alleles and their
112 underlying genomic events. The evolutionary scenario leading to the emergence of resistance in La
113 Réunion island is then discussed in regards of the worldwide distribution of resistance alleles and the
114 local demographic context. While providing a set of novel molecular markers to track insecticide
115 resistance in this mosquito vector, the present study contributes to anticipate the emergence of
116 insecticide resistance in the South-West Indian Ocean region and its consequences for vector control
117 strategies.

118

119 Results

120 Deltamethrin resistance alleles circulate in La Réunion island

121 In order to improve the identification of deltamethrin resistance alleles, an experimental design
122 combining field populations and the controlled selection of a composite line was used (**Fig. 1A,** see
123 methods). Comparative deltamethrin bioassays performed on three field populations confirmed the
124 presence of resistance alleles in La Réunion (**Fig. 1B**). The three field populations (Saint-Paul, Saint-
125 Louis and Sainte-Suzanne) showed a significant decreased mortality to deltamethrin compared with
126 the susceptible SRun reference line. As expected, the composite line maintained without deltamethrin
127 selection for 6 generations (NS line) showed a resistance level similar to field populations. Selecting
128 the composite line for 5 generations with deltamethrin (Sel line) resulted in its increased resistance as
129 compared to the NS line, suggesting that resistance alleles are not fixed in the field and have been
130 further selected by controlled-selection in the laboratory.

131

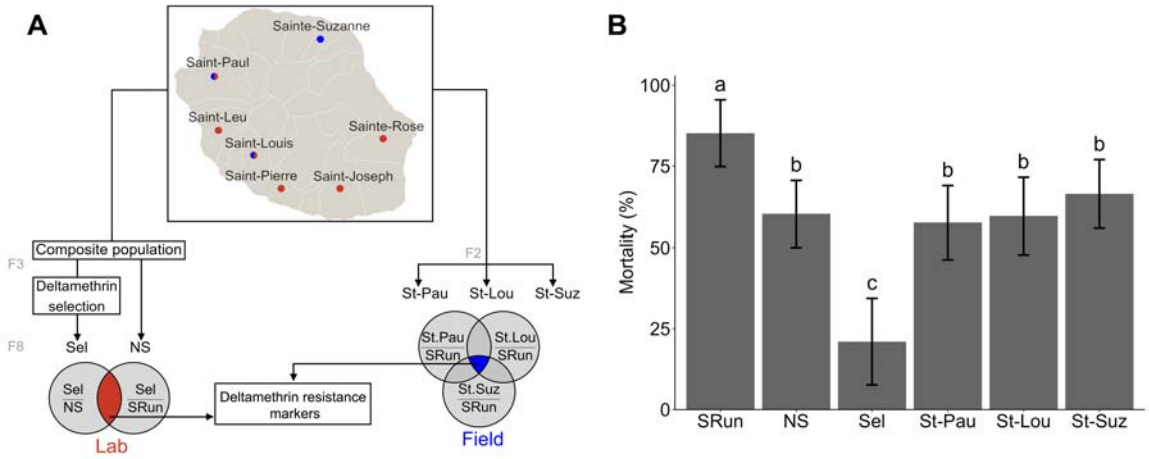

Fig 1. Study design and deltamethrin resistance levels. (A) Sampling sites and study design. The map shows the location of populations used to create the composite population from La Réunion island (red dots) and field populations (blue dots) used for analyses. For each line/population, the generation used is indicated. Venn diagrams illustrate the pairwise comparisons made for the identification of deltamethrin resistance markers (see methods). **(B)** Deltamethrin resistance levels. Mean mortality rates were obtained from standard WHO test tube assays using 0.03% deltamethrin impregnated papers. Error bars denote SD. Distinct letters indicate significantly distinct mortality rates (Conover-Iman test; N=9; p value ≤ 0.05). Sel: deltamethrin selected line; NS: non-selected line; St-Pau: Saint-Paul; St-Lou: Saint-Louis; St-Suz: Sainte-Suzanne; SRun: susceptible reference line from La Réunion.

The resistance phenotype is not associated with target-site mutations

Whole genome pool-seq data from all lines were used to screen for *Kdr* mutations affecting the VGSC gene encoding the biochemical target of deltamethrin. Among the 132 polymorphisms detected in coding regions, six were non-synonymous (**S1 File**), but none matched the position of *Kdr* mutations previously associated with pyrethroid resistance in *Ae. albopictus* (*i.e.* V410L, L982Y, S989P, I1011M, V1016G/I, I1532T, and F1534C: ,28). In addition, these six non-synonymous variants are unlikely to contribute to deltamethrin resistance as they do not show a frequency pattern consistent with deltamethrin resistance across all lines. Furthermore, they were located in cytosolic regions being distant from the protein domains carrying known *kdr* mutations. Altogether, this indicate that the detected protein variants are most likely neutral, and that *Kdr* mutation do not contribute to deltamethrin resistance in La Reunion island.

Resistance involves the over-transcription of detoxification enzymes

RNA-seq performed on adult females enabled the detection of 13,918 genes passing coverage threshold which included 697 resistance candidate genes. Differential transcription analysis identified 48 genes differentially transcribed in association with resistance when considering both lab and field comparisons (**Fig. 2A and S2 Table**). The 12 under-transcribed genes include a single candidate encoding an ABC-transporter (LOC109429564). Conversely, the 36 over-transcribed genes included 11

candidates, representing a significant enrichment compared with the global gene set (from 5% to 30.5%, X^2 test $p < 0.05$). All of them belong to three gene families classically involved in pyrethroid metabolism (P450s, transferases and ABC-transporters), leading to a significant enrichment of detoxification genes (from 54% to 100%, X^2 test $p < 0.05$; **Fig. 2B**). All over-transcribed candidate genes were located on chromosomes 1 and 2, some of them being clustered together (**Fig. 2C**). Several of them show high protein homology with genes previously involved in pyrethroid resistance in *Aedes aegypti* or *Anopheles gambiae*. The P450s *CYP6d5* (LOC115259486) was previously found over-transcribed in resistant *Ae. albopictus* populations from China (same gene named CYP6A8 in 47) and shows high homology with members of the CYP6Z subfamily previously involved in pyrethroid metabolism (60–62). The P450 *CYP6a14* (LOC109421559) shows high homology with members of the CYP6M subfamily validated as pyrethroid metabolizers in Anopheles mosquitoes (62,63). Similarly, *GST-1* (LOC109412993) and *GST4*-like (LOC109413318) showed high homology with *theta*- and *delta*-GSTs previously associated with pyrethroid in mosquitoes (45,64–67). Finally, the two ABC-transporters (LOC109407008 and LOC109429691) showed a high homology with the ABCC subfamily previously associated with pyrethroid resistance (68–73). Altogether, these results indicate that in absence of *Kdr* mutations, the deltamethrin resistance phenotype observed in La Réunion island is associated with an over-expression of detoxification enzymes likely involved in insecticide metabolism.

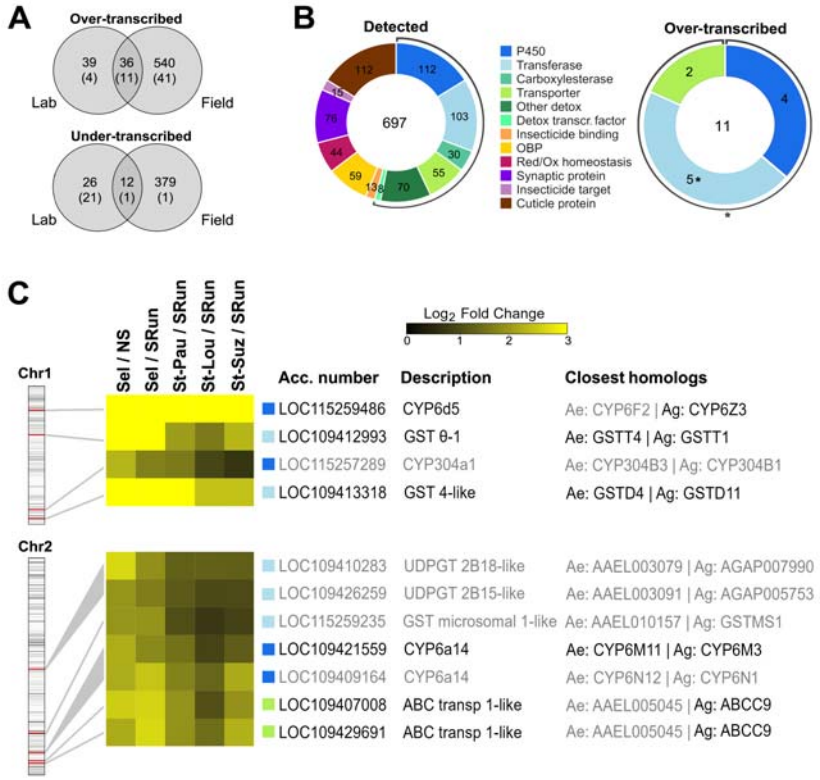

176 **Fig 2. Genes identified as differentially transcribed in association with deltamethrin resistance**. Only genes showing
177 consistent transcription level variations in both Lab and Field comparisons were considered associated with resistance (see
178 methods). **(A)** Venn diagrams showing the number of genes being differentially transcribed in association with resistance.
179 Numbers within brackets stand for candidate genes. **(B)** The left donut-chart describes all candidates genes detected by RNA-
180 seq and their respective gene families. The right donut-chart shows candidate genes associated with resistance. Black circular
181 arcs indicate gene families classically associated with detoxification. Stars indicate a significant enrichment from 'detected' to
182 'resistance associated' candidate genes (X^2 test, p value ≤ 0.05). **(C)** Candidate genes over-transcribed in association with
183 deltamethrin resistance. Log_2 fold changes obtained from each comparison are shown on the heatmap (scale from 0 to 3, see
184 S2 table for exact values). Colour squares refers to candidate gene families. Chromosomal positions are shown on the left
185 with the density of detected candidate genes shown as grey intensity. For each gene, NCBI accession number and description
186 are provided together with closest protein homologs in *Ae. aegypti* and *An. gambiae*. Genes in bold are those from which
187 close orthologs were previously associated with pyrethroid resistance. CYP: cytochrome P450; GST: glutathione S-transferase;
188 UDPGT: UDP-glycosyltransferase; ABC transp: ABC transporter; Sel: selected line; NS: non-selected line; St-Pau: Saint-Paul; St-
189 Lou: Saint-Louis; St-Suz: Sainte-Suzanne; SRun: susceptible reference line from La Réunion.

190 **Resistance is likely not associated with alternative splicing**

191 Using a *de novo* RNA-seq assembly strategy, we searched for alternative splicing events associated
192 with resistance. This analysis identified 166 events associated with resistance affecting 163 genes (**S3**
193 **Table**). This included 8 alternative splicing events, 4 large intron retention events (> 50 bp) though
194 none of them affected candidate genes. Such analysis also identified 161 short genomic indel events (≤
195 50 bp) among with two affected candidate genes: the transcription factor HR96 LOC109416347 (6 bp
196 indel) and the peroxiredoxin LOC109415663 (3 bp indel). Altogether, these data indicate that
197 resistance in la Réunion does not strongly rely on alternative splicing events.

198 **An over-transcribed P450 is likely affected by a genomic duplication**

199 As over-transcription can be caused by an increased copy number, whole genome pool-seq data were
200 used to identify genes affected by copy number variations (CNV) in association with resistance based
201 on their increased exonic read coverages (see Methods). This analysis identified 72 genes showing an
202 increased coverage associated with resistance. Five of them were also over-transcribed in resistant
203 lines including the P450 *CYP6d5* (**Fig. 3A and 3B; S4 Table**). Comparing normalized coverage profiles at
204 the *CYP6d5 locus* revealed an increased coverage in resistant lines, which supports the occurrence of a
205 ~60 Kb duplication (**Fig. 3C**). The putative breakpoints were poorly covered, likely due to the presence
206 of transposable elements which were annotated as a LTR element on the left and a Line/R1 element
207 on the right.

208

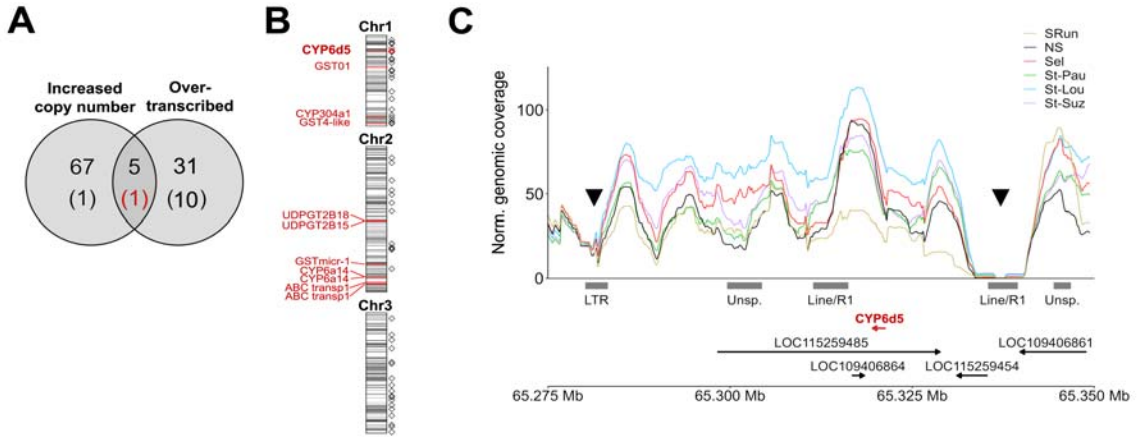

Fig 3. Gene copy number variant analysis. (A) Genes showing an increased copy number (CNV) in association with deltamethrin resistance in regards of those identified as overtranscribed. Numbers within brackets refer to candidate genes. **(B)** Distribution of gene copy number variants along chromosomes. Diamonds show the chromosomal position of the 72 genes showing an increased CNV associated with resistance. The red diamond refers to the candidate gene *CYP6d5* (LOC115259486). Over-transcribed candidate genes are named and shown as red marks in respect to candidate genes density (grey intensity). **(C)** Normalized read coverage profiles observed at the vicinity of *CYP6d5*. Normalized coverage profiles were computed for each line from whole genome pool-seq reads and smoothed using a 5 kb sliding window. The probable range of the duplicated region is delimited by black triangles. The *CYP6d5* gene is shown in red. Repeat masker annotation is shown as grey boxes. Genomic coordinates refer to AALBF3.v2 assembly. Sel: selected line; NS: non-selected line; St-Pau: Saint-Paul; St-Lou: Saint-Louis; St-Suz: Sainte-Suzanne; SRun: susceptible reference line from La Réunion.

Resistance is related to the selection of detoxification enzyme variants

Whole genome Pool-seq data were used to look for non-synonymous variants associated with resistance based on their frequency variation across resistant and susceptible lines. This analysis detected 197,403 non-synonymous variants passing coverage threshold with 11,679 of them affecting candidate genes (**Fig. 4A**). Among the 455 non-synonymous variants associated with resistance, 36 of them affected 27 distinct candidate genes **(Fig. 4B, S5 Table)**. A significant enrichment of candidate genes involved in detoxification was observed, mainly driven by a strong enrichment of P450s (from 15% to 33.3%, X^2 test $p < 0.02$). The 36 variants affecting candidate genes were spread over the three chromosomes (**Fig. 4C**). None of them affected over-transcribed genes though some were located in the same gene cluster. This was the case for the P450 *CYP6a8* variant located within a large CYP6 cluster which also include the two over-transcribed *CYP6a14* genes. Four major loci gathering multiple variants were identified in chromosome 3. The first one carried 4 variants affecting a *CYP4v2* and an ABC transporter. The second one included 9 variants affecting 6 P450s belonging to a cluster of 18 *CYP4C* genes. The last two gathered various candidate genes including a *CYP9f2* gene and an epoxide. Altogether, this analysis indicates that the deltamethrin resistance phenotype observed in La Réunion

236 is not only caused by the overtranscription of detoxification genes but also by the selection of protein
237 variants likely related to insecticide metabolism.
238

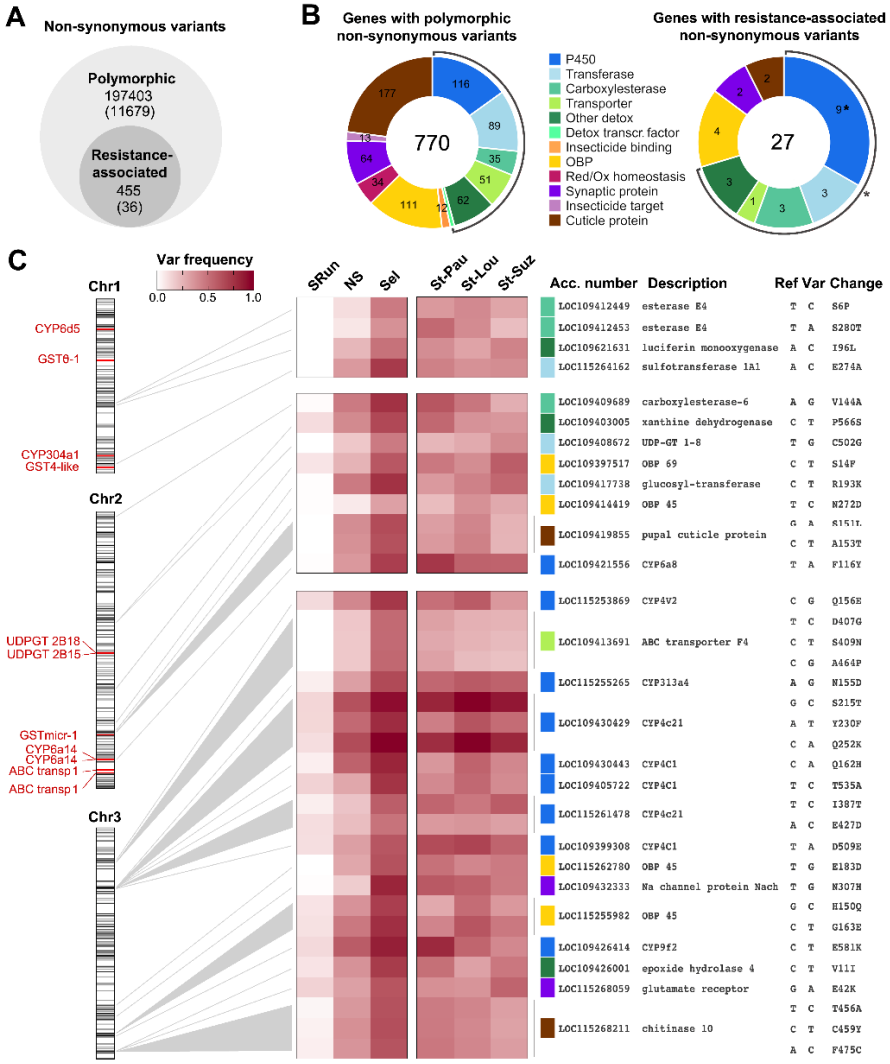

239
240

241 **Fig 4. Protein variants associated with resistance. (A)** Overview of non-synonymous variants identified. Numbers within
242 brackets refer to variants affecting candidate genes. Variants associated with resistance were identified based on allele
243 frequency variations across resistant and susceptible lines (see Methods) **(B)** The left donut-chart describes all candidate
244 genes from which polymorphic non-synonymous variants were detected. The right donut-chart described those associated
245 with resistance. Black circular arcs highlight gene families associated with detoxification. Stars indicate a significant
246 enrichment (X^2 test, p value ≤ 0.05). **(C)** Candidate genes with non-synonymous variants associated with resistance. The heat
247 map shows the frequency of the variant allele across all lines. The chromosomal position of each variant is shown on the left
248 in respect to over-transcribed candidate genes (red marks) and candidate gene density (grey intensity). For each variant, gene
249 family (colour square), gene accession number, gene description, nucleotide and amino-acid change are indicated. CYP:
250 cytochrome P450; GST: glutathione S-transferase; UDPGT: UDP-glycosyltransferase; ABC transp: ABC transporter; Sel:

251 selected line; NS: non-selected line; St-Pau: Saint-Paul; St-Lou: Saint-Louis; St-Suz: Sainte-Suzanne; SRun: susceptible
252 reference line from La Réunion.

253

254 **Over-transcribed detoxification genes are not under direct selection**

255 Exonic polymorphism data were then used to look for gene-based selection signatures across the
256 genome between the Sel and NS lines based from allele frequency differentiation indexes (see
257 Methods). Among the 11 over-transcribed candidate genes, only the P450 *CYP304c1* and the
258 microsomal *GST-1* showed high differentiation indexes, which supports their cis-regulation. Other
259 over-transcribed candidate genes were below the baseline, consistent with their trans-regulation (**Fig.**
260 **5A**). Conversely, most candidate genes carrying protein variants associated with resistance showed
261 high gene differentiation indexes, supporting selection acting on the same *loci*. Among candidate
262 genes, those showing the highest differentiation indexes included two carboxylesterases *E4-like* on
263 chromosome 1, two UDPGTs and the *CYP6a8* P450 on chromosome 2, and the ABC transporter *F4* and
264 the two *CYP4c1* P450s on chromosome 3. Overall, though genetic drift may have occurred between
265 the Sel and NS lines, the high differentiation indexes observed across the three chromosomes support
266 the hypothesis of a multigenic adaptation based on standing genetic variation in La Réunion island (**Fig.**
267 **5B**).

268 **An inverted superlocus is under deltamethrin selection in La Réunion**

269 This analysis also identified a hundred genes located within an intriguing region of chromosome 2
270 displaying very high differentiation levels (**Fig. 5C and S6 Table**). This large 9.6 Mb *locus* showed a
271 strong selection signal in the Sel/NS comparison but also in other 'resistant *vs* susceptible'
272 comparisons coherent with a low recombination rate. Indeed, a quarter of the 3141 non-synonymous
273 polymorphisms detected in this region are above the whole genome top centile for Sel/NS
274 differentiation indexes. Examining reads topology identified 'one mate swap' read pairs and split reads
275 supporting the presence of a large genomic inversion whose breakpoints were 120,519,062 and
276 130,178,023. The partial mapping of these reads at the breakpoints together with the unmapped
277 fragments matching to multiple genomic locations supported the flanking of this inversion by two
278 transposable elements. The presence of this inversion at low frequency in the susceptible reference
279 strain SRun also suggests its pre-existence prior to its selection by deltamethrin in La Réunion. Among
280 the 107 genes located within the inverted region, only four belong to candidate genes including two
281 ABC-transporters, a cytochrome b5-like and a cuticle protein. However, none of them were
282 differentially transcribed, affected by CNV, or carried non-synonymous variants associated with
283 deltamethrin resistance. Among other genes located within the inversion, none showed a clear
284 association with a known resistance mechanism. Fifteen genes encoded known or putative (*i.e.* zing

finger proteins) transcription factors although none were previously associated with detoxification enzymes regulation. Several polymorphisms showing the highest Sel/NS differentiation affected the uncharacterized gene LOC115268503. Protein homology suggest that this gene encodes a S/T protein phosphatase with ankyrin motifs. As the voltage-gated sodium channel targeted by pyrethroids can be regulated by phosphorylation and interact with ankyrins (74,75), this gene is an attractive candidate to explain the selection of this large inversion by deltamethrin.

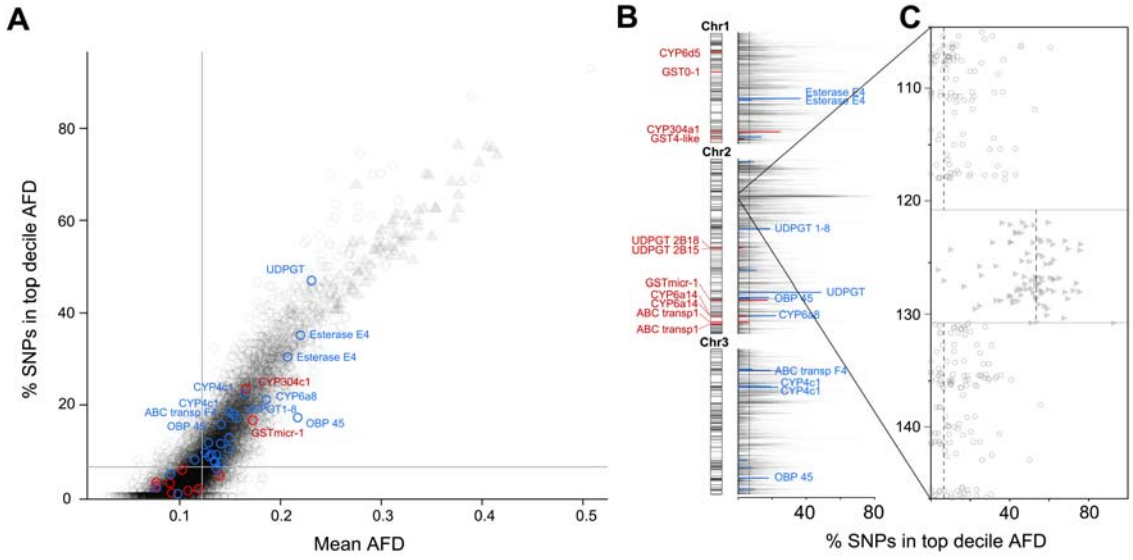

Fig 5. Genome-wide allele frequency differentiation. (A) The plot shows two genetic differentiation indexes for the Sel/NS line comparison: the mean Allele Frequency Difference per gene (mean AFD, absolute value) and the proportion (%) of SNPs per gene showing an AFD within the top decile of the global distribution (% SNPs in top decile AFD). These differentiation indexes were computed for the 10,192 protein-coding genes carrying > 20 bi-allelic substitutions (see Methods). Median values are shown as grey lines. Candidate genes within top quartiles for both differentiation indexes are annotated with those differentially transcribed in association with resistance in red and those carrying protein variants associated with resistance in blue. Triangles denotes genes carried by the genomic inversion identified in chromosome 2. **(B)** Genome wide overview of the '% SNPs in top decile AFD' index for the Sel/NS comparison. The dashed line stands for the median of the differentiation index across all genes. The chromosomal position of candidate genes associated with resistance is shown together with candidate gene density (grey intensity). **(C)** Focus on the genomic region carrying the 9 Mb inversion associated with resistance. The '% SNPs in top decil AFD' index is shown for all genes. Horizontal grey lines delimit the inverted region with breakpoints at Chr2:120,519,062-130178023 in AALBF3.v2 assembly (Chr2:405,097,032-416,198,432 in AALBF5 assembly). Vertical dashed lines show the median of the '% SNPs in top decile AFD' index within and outside the inverted region. The genomic scale is in Mb respective to AALBF3v2.

Discussion

Metabolic resistance likely emerged from local adaptation in La Réunion island

309 Bioassays performed on field mosquito populations from La Réunion island revealed a significant
310 deltamethrin resistance phenotype, confirming the rise of resistance observed since 2017 (58).
311 Considering that resistance may have remained undetected for some times, the emergence of
312 resistance may have begun a few years after deltamethrin was adopted for vector control following
313 the 2005-2006 chikungunya outbreak. The resistance level of the non-selected composite line was
314 similar to those observed in the field, suggesting that the sampling design was efficient at capturing
315 resistance alleles circulating in the island. Indeed, the ancient colonization of this insular territory by
316 *Ae. albopictus* was linked to a high local genetic diversity with significant gene flows between
317 populations (76–78).

318 More than 30 non-synonymous polymorphisms affecting the VGSC targeted by deltamethrin have
319 been identified in *Ae. albopictus* worldwide but only a few were consistently associated with
320 pyrethroid resistance (23,26,28,79: V1016G, I1532T and F1534S/C/L). Despite the sequencing of large
321 mosquito pools at high coverage, none of these *Kdr* mutations was detected in La Réunion island,
322 either in field populations or in composite laboratory lines. Considering the recurrent usage of
323 deltamethrin since 2005, this supports the absence of *Kdr* mutations in La Réunion at the time of the
324 study. As *Kdr* mutations have already spread across multiple continents including Asia, Europe and
325 Africa (26,28), such result also confirm that limited gene flow occurred from these regions. Instead, a
326 multigenic metabolic resistance phenotype was observed, involving detoxification genes belonging to
327 families involved in pyrethroid metabolism such as cytochrome P450s, glutathione S-transferases,
328 UDP-glycosyl transferases, and ABC-transporters (31,80). Elevated detoxification enzyme activities
329 have been linked to deltamethrin resistance in *Ae. albopictus* populations from various regions (46,81–
330 84).

331 Transcriptomic screenings revealed the over-transcription of the same detoxification gene families in
332 *Ae. albopictus* resistant populations from Asia with some P450s being functionally validated (44,45,47).
333 Among the detoxification genes identified in La Réunion, only the P450 (CYP6d5) was previously
334 identified as contributing to deltamethrin resistance in *Ae. albopictus* (same CYP gene named CYP6A8:
335 47). Yet, several of them showed high protein homology with known pyrethroid resistance genes
336 identified in other mosquito species. This includes two P450s showing high homology with
337 *CYP6Ms/CYP6Zs* subfamilies, two GSTs likely belonging to GST-theta and -delta families and two ABC-
338 transporters likely belonging to the ABCC family. Although functional validation is needed to clarify
339 their importance in the overall phenotype, the emerging picture is the independent selection of
340 detoxification genes in Asia and La Réunion. Such hypothesis is also supported by the absence of *Kdr*
341 mutations previously detected in Asia in La Réunion island. Such parallel evolution of detoxification
342 genes under pyrethroid selection is probable considering the functional redundancy observed within

343 these gene families whose members are often organized in clusters of genes sharing a high homology
344 (10,85). Altogether, while the introgression of metabolic resistance alleles cannot be ruled out, the
345 genetic isolation of La Réunion island together with the absence of *Kdr* mutations and the specific
346 nature of the genes identified support their local selection from standing genetic variation.

347 **Multiple genetic events underly the resistance phenotype**

348 Gene duplications mediating the over-expression of detoxification genes have been frequently
349 associated with the rapid adaptation of mosquitoes to insecticides (32,35,86,87). Here, the over-
350 transcribed P450 *CYP6d5* was linked to the presence of a ~100 Kb genomic duplication. Although our
351 short-read Pool-seq data did not allow to fully resolve the genomic architecture of the duplicated
352 locus, its flanking by transposable elements (TEs) was not surprising as TE-movements are often
353 associated with genomic duplication events (86,88), especially in TE-rich genomes such as *Aedes*
354 mosquitoes (89–91). No such duplication was identified for the other over-transcribed detoxification
355 genes, implying that their over-transcription is rather mediated by cis- or trans-regulation. In this
356 regard, the nuclear receptors CncC/Maf and AhR-ARNT considered as key regulators of insect
357 detoxification genes (92) were not differentially transcribed nor affected by protein variants in
358 association with resistance. Nevertheless, a two-codons deletion variant affecting the transcription
359 factor HR96 showed an increased frequency in resistant lines. The contribution of this transcription
360 factor to the regulation of detoxification enzymes has been demonstrated in spider mites (93,94).
361 Although this requires further validation, this finding supports the potential role of HR96 in the
362 regulation of detoxification enzymes in *Ae. albopictus*.

363 As metabolic resistance may also be the consequence of the selection of proteins variants showing a
364 higher activity toward the insecticide (10), polymorphism data were screened for non-synonymous
365 variants associated with resistance. Such analysis identified multiple detoxification protein variants
366 with P450s being over-represented. Yet this gene set showed no overlap with over-transcribed genes,
367 suggesting that these two adaptive mechanisms contribute to the multigenic resistance phenotype
368 observed in La Réunion island. Indeed, in a context of local adaptation, it is expected that selection
369 retains any polymorphism that contribute to resistance, affecting both gene expression and protein
370 function. Of particular interest was the selection of multiple P450 variants belonging to a cluster of 18
371 *CYP4C-like* genes on chromosome 3. Indeed, while *CYP4s* are not considered as classical xenobiotic
372 metabolizers in mosquitoes as opposed to *CYP6s*, *CYP9s*, some of them have been shown to be over-
373 transcribed in association with pyrethroid resistance in *Ae. aegypti* (95), suggesting their possible
374 contribution to deltamethrin metabolism. Similarly, the identification of two carboxylesterase variants
375 associated with resistance may indicate that these enzymes can still be active on deltamethrin or its

376 metabolites, even though the cyano group of type II pyrethroids like deltamethrin is thought to protect
377 the ester bond from a direct hydrolysis (96).

378 Polymorphism data were then used to look for genes under positive selection in association with
379 resistance. As expected, a good proportion of detoxification protein variants associated with resistance
380 showed a positive selection signal at the gene level. On the other hand, apart from one P450 and one
381 GST, most over-transcribed detoxification genes showed poor selection signals, supporting their trans-
382 regulation. Unexpectedly, such analysis also identified a large ~9 Mb genomic inversion on
383 chromosome 2 behaving as a supergene under deltamethrin selection. Genomic inversions can play a
384 key role in local adaptation as demonstrated in various biological models (97–100). Whether this
385 genomic event is specific to the South-West Indian Ocean or more widely distributed remains to be
386 investigated. In that concern, the identification of the inversion breakpoints will facilitate its high-
387 throughput genotyping by PCR. The hundred genes carried by the inverted locus included four
388 candidates but none of them were directly associated with deltamethrin resistance, suggesting that
389 they do not drive its selection. Considering the strong genetic linkage of the inverted haplotype,
390 deciphering which gene(s) drive the selection of this supergene is not at reach from the current data
391 set and requires functional approaches.

392 **A warning bell for the South-West Indian Ocean**

393 The French territory of La Réunion island is a hotspot of arbovirus transmission in the South West
394 Indian Ocean in line with a high human density and the presence of *Ae. albopictus* (57). Such
395 epidemiological context led to the recurrent use of deltamethrin for vector control since the first
396 Chikungunya outbreak of 2005-2006. In a context of genetic isolation, this repeated insecticide
397 pressure resulted in the local selection of a metabolic resistance phenotype underlain by various
398 genetic events. Such evolutionary scenario is supported by the multigenic nature of the phenotype
399 together with the striking absence of *Kdr* mutations, which are already widely distributed in this
400 species (26,28). At the time of the study, the resistance phenotype observed in the field was moderate
401 and can be further increased following a few generations of deltamethrin exposure, suggesting that
402 the selection of resistance alleles is undergoing in La Réunion and might be counterbalanced with
403 fitness costs. As the selection of this multigenic resistance phenotype may affect various mosquito life
404 traits including vector competence (7,101), precising its impact on population dynamics and viral
405 transmission is of interest.

406 Considering that the selection process was undergoing by the time of the study, the intense vector
407 control activity associated with recent chikungunya and dengue outbreaks may have resulted in an
408 increased frequency of resistance alleles in La Réunion and their dispersal to other neighbouring
409 territories of the South-West Indian Ocean. In addition, although *Kdr* mutations were not detected by

410 the time of the study, their introduction from Europe, Asia or Africa should be considered as a major
411 risk for the region. Indeed, their introduction in populations already carrying metabolic alleles is
412 expected to lead to an additive resistance phenotype that may impact vector control efficacy, as
413 shown in *Ae. aegypti* (19,21). In this context, the present study calls for an improved surveillance of
414 pyrethroid resistance in this region. Ideally, this surveillance should combine annual bioassays on
415 sentinel populations and the tracking of key metabolic resistance alleles identified here together with
416 known *Kdr* mutations.
417

418 ## Methods

419 **Mosquito lines and experimental design**

420 All mosquito lines were maintained under standard insectary conditions (27 ± 2°C, 70 ± 10 % relative
421 humidity and light/dark cycle 14h:10h). Populations size were maintained over 1000 individuals to
422 reduce the effect of genetic drift. Larvae were reared in tap water and fed with hay pellets. Adults
423 were maintained in mesh cages and fed on filter papers impregnated with a 10 % honey solution.
424 Blood feeding was conducted on mice to generate eggs of the next generation. Three days-old non-
425 blood-fed adult females were used for bioassays and molecular work.

426 The experimental design combined different mosquito populations all originating from La Réunion
427 island (**Fig. 1A**). First, a composite population from la Réunion island was created by pooling >500
428 larvae from six field populations collected in 2018-2019 using a minimum of three ovitraps per
429 population. After two generations of genetic mixing (F1 to F3), the composite population was split in
430 two separated lines (N>1000 in each line): the first being maintained without insecticide selection (NS
431 line) and the other being selected with deltamethrin for five successive generations (Sel line). Selection
432 was conducted on males and females separately prior mating as follows. Batches of 25 non-blood-fed
433 3-5 days-old adults were exposed to filter papers impregnated with 0.03% deltamethrin using WHO
434 test tubes. Exposure times were adjusted from 30 min to 1h to reach 40-60% mortality for each sex.
435 Surviving males and females were then pooled in a single mesh cage and allowed to reproduce.
436 Females were blood fed and allowed to lay eggs to generate the next generation. Three field
437 populations sampled in 2021 from the localities of St-Paul, St-Louis and St-Suzanne were also used.
438 Finally, the laboratory susceptible strain SRun colonized from La Réunion island in the 2000s was used
439 as reference line. For molecular analyses, genes and polymorphisms associated with resistance were
440 identified based on the five pairwise comparisons: 'Sel *vs* NS'; 'Sel *vs* SRun' and 'each field population
441 *vs* SRun'. Only genes and polymorphisms showing consistent variations (in the same direction) for all
442 comparisons were retained.

443 **Bioassays**

444 Comparative deltamethrin bioassays were performed on 3-5 days-old adult females following WHO
445 mosquito testing guidelines (102) using test tubes equipped with home-made insecticide papers
446 impregnated with 0.03% deltamethrin. Each bioassay was conducted using 9 replicates of 25 females
447 and an exposure time of 1h. Such insecticide dose resulted in a mortality >80% in the susceptible
448 reference line SRun. After insecticide exposure, mosquitoes were allowed to recover for 24h with a
449 cotton bowl impregnated with a 10% honey solution before mortality recording.

450 **Reference genome and candidate genes**

451 Genomic analyses were performed using the version AALBF3 of *Ae. albopictus* reference genome,
452 which was the latest available assembly at the time of this study (103). As this assembly was made
453 from 574 ordered scaffolds, the successive scaffolds were assembled into pseudo-chromosomes with
454 50N spacers (hereafter referred to as AALBF3.v2 assembly). A gff3 annotation file based on AALBF3.v2
455 assembly was also created based on AALBF3 annotation. The genomic coordinates of each scaffold on
456 AALBF3.v2 assembly is provided in **S7 Table**. Among the 22,435 features annotated in AALBF3.v2, only
457 the 17,342 genes and pseudogenes carried by the three nuclear chromosomes were retained for
458 genomic analyses. A subset of 953 genes belonging to 12 different families possibly involved in
459 insecticide resistance was defined. These candidate genes included: insecticide targets; synaptic
460 proteins; detoxification enzymes *sensu lato*; known detoxification transcription factors; ABC-
461 transporters; insecticide binding proteins; cuticle proteins; red/ox enzymes; odorant binding proteins
462 (**S8 Table**).

463 **RNA-sequencing**

464 For each line, four RNA-seq libraries were prepared from distinct batches of 25 five days-old non-
465 blood-fed females. Total RNA was extracted using TRIzol® (ThermoFisher Scientific) according to
466 manufacturer's instructions. RNA extracts were quantified with a Nanodrop One (ThermoFisher
467 Scientific) and diluted to meet sequencing requirements. Sequencing was performed by the BGI
468 Hongkong Tech Solution NGS Lab. Sample quality control was conducted on an Agilent 2100 and
469 libraries were prepared from 10 ng total RNA following the DNB-seq Eukaryotic Strand-specific mRNA
470 library protocol. Briefly, mRNAs were enriched with poly-A tails using oligodT beads and fragmented to
471 an average size of 200-400 bp before being reverse transcribed using random primers. Double-
472 stranded cDNAs were end-repaired and 3' adenylated. Adaptors were ligated at the 3'-end of the
473 cDNAs. Libraries were PCR amplified using rolling circle amplification to make DNA nanoballs (DNB)
474 and sequenced in multiplex as 100 bp paired-end reads. Adapters were trimmed with the SOAPnuke
475 v2.2.1 (104) and reads were filtered on base quality to reach an average Phred+33 score of 37. Quality

476 control was conducted using FastQC (105) leading to an average of 60.2 M quality-filtered reads per
477 replicate. Reads were then mapped onto the AALBF3.v2 assembly using STAR v2.7.10a (106) with
478 default parameters, except a minimum intron size of 10 bp. Mapping quality was assessed with
479 samtools v1.6 (http://www.htslib.org/), with an average of 94 % of reads being properly mapped (**S9**
480 **Table**). Gene read counts were quantified by STAR with default parameters.

481 *Differential transcription*

482 Differential transcription analysis was performed using DESeq2 (Love et al., 2014) on all genes and
483 pseudogenes showing ≥5 read counts in each of the four replicates for at least one mosquito line.
484 Differentially transcribed genes were identified based on their congruent transcription fold change (FC)
485 and adjusted Student' t-test *p* values (False Discovery Rate for multiple testing correction, 107) across
486 the five 'resistant vs susceptible' comparisons (see experimental design on **Fig. 1**). Fold change
487 thresholds were set as follows: FC ≥ 3 in 'Sel vs NS'; FC ≥ 3 in 'Sel vs SRun' and FC ≥ 1.5 in the three
488 'field vs SRun' comparisons while adjusted *p* Value threshold was set to 0.001 for all comparisons. In
489 order to clarify the role of detoxification genes over-transcribed in association with resistance, their
490 closest homologs were identified in *Ae. aegypti* and *An. gambiae* using a protein blast against *Ae.*
491 *aegypti* (LVP_AGWG) and *An. gambiae* (PEST) proteomes from VeuPathDB (108,109). As P450 gene
492 descriptions and gene names can vary across different genome versions, blast results were backed up
493 with a phylogenetic analysis performed on *CYP6s* protein sequences from *Ae. albopictus, Ae. aegypti*
494 and *An. gambiae*. Protein sequences were retrieved from NCBI and those having a validated role in
495 pyrethroid resistance were identified based on the literature and sequence alignments. Phylogenetic
496 trees were built using the only 'NGPhylogeny.fr' pipeline using approximate likelihood-ratio test (aLRT)
497 as branch support, with a *CYP4* sequence as outgroup (110).

498 *Alternative splicing*

499 Alternative splicing events and indels were identified from RNA-seq data using KisSplice v2.6.2 (111).
500 This *de novo* splicing events predictor was run on each replicate of each line with default parameters,
501 except the parameter -b which was set to 15 to account for the higher level of polymorphism in *Ae.*
502 *albopictus* compared with mammals. Splicing variants were identified with KissDE R package v1.19.0
503 (112). Only variants covered by at least 20 reads, affecting known genes and showing a congruent
504 splicing variation across all 'resistant vs susceptible' comparisons were retained. Delta Percent Spliced
505 In (ΔPSI) threshold were as follows: 20% for 'Sel *vs* NS'; 20% for 'Sel *vs* SRun' and 15% for the three
506 'field *vs* SRun' comparisons. The adjusted *p* value threshold was set to 0.05 (Benjamini & Hochberg
507 FDR for multiple testing correction). The splicing events passing these filters were then mapped to
508 AALBF3.v2 assembly using KisSplice2RefGenome v1.2.3

509 (https://kissplice.prabi.fr/tools/kiss2refgenome/) and assigned into three types: alternative splicing,
510 indels and intron retentions. The distinction between genomic indels and intron retention was based
511 on an arbitrary threshold (indel if ≤ 50 bp and intron retention if > 50 bp).

512 **Whole genome pool sequencing**

513 For each line, three batches of 33-35 three days-old virgin non-blood-fed females were sampled for
514 whole genome pool-sequencing (100 individuals per line). Genomic DNA was extracted separately for
515 each batch using the GENTRA Puregene kit (QIAGEN) following manufacturer's instructions quantified
516 using Qubit (Qiagen) and then pooled in equal DNA quantity. After quality check, one sequencing
517 library was prepared for each line following the DNBseq plant and animal whole genome resequencing
518 protocol (https://en.mgi-tech.com/products/). Briefly, DNA was fragmented, size selected (insert size
519 ~350 bp) and end-repaired. Adapters were ligated to the DNA fragments which were then size-
520 selected, amplified by PCR using rolling circle amplification and sequenced in multiplex as 150 bp
521 paired-end reads with the DNBseq Technology (MGI Tech Co). Sequencing reads were filtered based
522 on base quality resulting in a final average Phred score of 37 and adapters were removed with the
523 SOAPnuke software v2.2.1 (104) leading to an average of ~1630 M reads per line (**S9 Table**). Reads
524 were then mapped onto the *Ae. albopictus* AALBF3.v2 genome with BWA mem v0.7.17-r1188 (113).
525 SAM files were converted into BAM format, sorted by coordinates and unmapped reads were removed
526 using samtools v 1.6 (114). Mapped reads were trimmed and only reads showing a probability of
527 correct mapping of 0.999 were kept (MapQ ≥30). PCR duplicates were removed using picard
528 MarkDuplicates v2.27.5 (http://broadinstitute.github.io/*picard*), resulting in an average of 631 M
529 mapped reads per sample and a mean genome coverage of 64.2X.

530 *Copy number variations*

531 Genomic duplications were searched for by looking for genes showing a higher mean read coverage in
532 resistant than in susceptible mosquito lines. Though likely to generate false positives, this approach
533 was preferred to pipelines integrating local coverage variations and the presence of flanking non-
534 colinear reads (115) because the *Ae. albopictus* is genome is highly enriched with transposable
535 elements (>41% of the genome, 89) likely to generate false negatives. Indeed, transposable elements
536 are frequent at duplication breakpoints leading to the loss of non-colinear reads (*e.g.* split reads and
537 both mate flip reads) due to multiple mapping events. Since intronic regions are highly variable and
538 thus more subject to local coverage variations, mean normalized gene coverages were computed from
539 exonic regions only. Fold changes of normalized exonic coverage between lines were computed for all
540 genes. Since very low gene coverage can lead to artefactual high coverage variations, genes showing a
541 normalized coverage lower than the 5% global quantile were not considered. Furthermore, a global
542 observation of the data set indicated that the dispersion of coverage variations increased for smaller

543 transcripts. To take this into account, a sliding windows approach considering transcript length was
544 applied to identify differentially covered genes: for each pairwise line comparison, a gene was
545 considered as affected by a positive copy number variation (CNV) when its normalized coverage
546 variation was higher than the 95% quantile of the variation observed from the 1000 genes showing the
547 most similar transcript lengths. Following this approach, genes were considered as showing a positive
548 CNV associated with resistance when passing this threshold for all 'resistant vs susceptible'
549 comparisons ('Sel *vs* NS', 'Sel *vs* SRun' and the three 'field *vs* SRun' comparisons).

550 *Gene polymorphisms*

551 Gene polymorphisms associated with resistance were searched for using reads mapped to the coding
552 regions of protein-coding genes. For each line, polymorphisms were called using bcftools-v1.17 (116).
553 We then retained biallelic variants showing a read coverage between 50 and 300 reads in all lines, a
554 frequency ≥ 15% in at least one line and a frequency variation ≥ 15% between at least two lines. Genic
555 effects were annotated according to the longest reading frame using snpEff v5.2c (117). As the
556 reference genome *Foshan* strain is susceptible to deltamethrin (118) variants were considered
557 associated with resistance if the frequency of the variant allele increased in 'resistant vs susceptible'
558 comparisons. Frequency thresholds were as follows: frequency ≤ 15% in the susceptible SRun line,
559 frequency variation ≥ 25% in 'Sel *vs* SRun' and in 'Sel *vs* NS' comparisons, and frequency variation ≥
560 20% in the three 'Field *vs* SRun' comparisons.

561 We also specifically searched for non-synonymous polymorphisms affecting the gene encoding the
562 voltage-gated sodium channel protein targeted by deltamethrin (VGSC-para gene carrying the Kdr
563 mutations). However, this gene was incorrectly assembled in AALBF3 likely due to uncontrolled
564 heterozygosity. Indeed, the previous AALFBF2 assembly (Palatini et al., 2020) contains two annotated
565 gene copies, each located in a different scaffold (the 'VGSC-para' LOC109421922, and the 'VGSC para-
566 like' LOC109432678*)*. In AALBF3, both genic sequences were present but the 'para' sequence was not
567 annotated as a gene. In the latest AALBF5 assembly, a better control of heterozygosity led to the two
568 contigs being merged, resulting in a single annotated 'VGSC-para' gene (LOC109421922). We therefore
569 assumed that the AALBF5 assembly is correct. In order to study the polymorphism of this gene, all
570 reads mapped to AALBF3.v2 in the *para* (Chr3:378648962-378932310) and *para-like* regions
571 (Chr3:377089613-377411247) were re-mapped to the AALBF5 gene LOC109421922 and SNPs were
572 called as described above.

573 *Selection signatures*

574 Polymorphisms data were also used to look for selection signatures associated with deltamethrin
575 resistance between the Sel and NS lines, which only diverged by 5 generations of deltamethrin

576 selection. This analysis was based on all exonic bi-allelic substitutions covered by 50 to 300 reads in
577 each line and being polymorphic between these two lines (*i.e.* showing a variant frequency from 5% to
578 95% in at least one line). From this dataset, two genetic differentiation indexes were computed at the
579 gene level: the mean Absolute Frequency Difference (mean AFD), and the percentage of SNPs in the
580 top decile of the overall genomic AFD distribution. These indexes were plotted against each other and
581 across the AALBF3.v2 genome for the 10192 protein-coding genes containing ≥ 20 substitutions.

582

583 ## Acknowledgments

584 This study was funded by the French Agency for Food, Environmental and Occupational Health &
585 Safety under the grant number EST-19-055. TB was supported by a PhD fellowship funded by the
586 Grenoble-Alpes University (UGA). The funders had no role in study design, data collection and
587 interpretation, or decision to submit the work for publication. We thank Dr. Julien Cattel for providing
588 the susceptible reference strain SRun. We also thank Vincent Lefort for help with phylogenetic
589 analyses.

590

591 ## Data availability

592 RNA-seq and WG Pool-seq sequencing data have been deposited at EBI short read archive (SRA) under
593 accession numbers E-MTAB-15418 and E-MTAB-15456.

594

595 ## Ethical aspects

596 Mice were kept in the animal facility of the Biology department of the University of Grenoble-Alpes,
597 approved by the French Ministry of Animal Welfare (agreement no. B 38 421 10 001) and used in
598 accordance with the laws of the European Union (directive 2010/63/EU). The use of animals for this
599 study was approved by the ComEth Grenoble-C2EA-12 ethics committee mandated by the French
600 Ministry of Higher Education and Research (MENESR). The study was conducted in accordance with
601 the ARRIVE guidelines.

602

603 ## Author contributions

604 **Conceptualization:** Tiphaine Bacot, Jean-Marc Bonneville, Jean-Philippe David
605 **Data curation:** Tiphaine Bacot, Pascal Oberbach, Vincent Lacroix, Jean-Marc Bonneville

606 **Formal analysis:** Tiphaine Bacot, Pascal Oberbach, Jean-Marc Bonneville, Jean-Philippe David
607 **Funding acquisition:** Jean-Philippe David
608 **Investigation:** Tiphaine Bacot, Pascal Oberbach, Thierry Gaude, Louis Nadalin, Frederci Laporte,
609 Guillaume Dupuy, Frederic Boyer
610 **Methodology :** Frederic Boyer, Vincent Lacroix, Tiphaine Bacot, Jean-Marc Bonneville, Jean-Philippe
611 David
612 **Project administration:** Jean-Philippe David
613 **Resources:** Nausicaa Habchi-Hanriot, Guillaume Dupuy, Cyrille Czeher
614 **Supervision:** Jean-Marc Bonneville and Jean-Philippe David
615 **Writing – original draft:** Tiphaine Bacot, Vincent Lacroix, Jean-Marc Bonneville, Jean-Philippe David
616 **Writing – review & editing:** Tiphaine Bacot, Michael C Fontaine, Jean-Marc Bonneville, Jean-Philippe
617 David
618

619 ## Supporting information

620

621 **S1 File. Polymorphisms in the VGSC gene.** The first xlsx sheet describes all polymorphisms detected in
622 the VGSC coding regions. For each polymorphism, the following information is provided: Position
623 relative to AALBF5 assembly; amino-acid position in respect to the longest isoform; genic effect;
624 variant allele frequency in each line; Variant allele frequency variations between resistant and
625 susceptible lines; number of reads supporting each allele for each line. The second xlsx sheet provides
626 a graphical overview of the position of the variant identified relative to transmembrane domains and
627 known Kdr mutations.

628 **S2 Table**. **Gene transcription data.** This table describes transcription data for all genes detected by
629 RNA-seq. For each gene the following information is provided: AALBF3 accession number;
630 chromosomal position relative to AALBF3.v2 assembly; coding strand; gene type; Candidate gene
631 family; baseMean (mean normalized read counts across all conditions); $\log_2$ fold change and adjusted P
632 value for each resistant/susceptible comparison.

633 **S3 Table. Alternative splicing.** For each splicing event identified, the following information is provided:
634 AALBF3 accession number; gene description; candidate gene family; chromosome; event start; event
635 end; event type and subtype; event size in bp; frameshift occurrence; mean coverage; percent spliced
636 in (PSI for each line); PSI variation (ΔPSI for each comparison).

637 **S4 Table. Gene copy number variations.** For each gene detected, the following information is
638 provided: AALBF3 accession number; chromosomal position relative to the AALBF3.v2 assembly;

coding strand; gene type; candidate gene family; gene description; mRNA length; normalized exonic coverage (for each lines); mean normalized coverage across all lines; coverage filter; CNV status for both lab and field comparisons.

S5 Table. Non-synonymous variants associated with resistance. For each variant, the following information is provided: chromosomal position relative to AALBF3.v2 assembly; reference and variant alleles; polymorphism type; AALBF3 gene accession number; gene description; candidate gene family; longest transcript; variant exon rank; variant genic effect; amino-acid change; cDNA position relative to cDNA length; amino-acid position relative to protein length; total coverage (for each line); variant allele frequency (for each line).

S6 Table. Gene differentiation indexes. For each gene the following information is provided: Gene accession number; chromosomal position relative to AALBF3.v2 assembly; coding strand; gene description; candidate gene family; total number of polymorphic SNPs; number of synonymous SNPs; number of non-synonymous SNPs; number of resistance-associated non-synonymous SNPs; mean Allele Frequency Variation between Sel and NS Lines (mean AFD); the percent of SNPs showing an AFD within the top decile of the global distribution (% top decil AFD); differential transcription associated with resistance (Yes/No); gene being within the inversion identified on chr2 (Yes/No).

S7 Table. The AALBF3.v2 genome assembly. The genomic position of AALBF3 scaffolds on AALBF3.v2 chromosomes is provided. AALBF3 scaffolds were assembled in the same order as described in Boyle et al. 2021 with 50N spacers inserted between them.

S8 Table. Resistance candidate genes. For each gene the following information is provided: AALBF3accesion number; chromosomal position relative to AALBF3.v2 assembly; coding strand; gene type; candidate gene family; gene description.

S9 File. Sequencing data overview. The first xlsx sheet provides RNA-seq sequencing and mapping statistics. The second xlsx sheet provides whole genome Pool-seq sequencing and mapping statistics.

References

1. Orr HA. The genetic theory of adaptation: a brief history. Nat Rev Genet. 2005;6(2):119–27.

2. Hendry AP, Farrugia TJ, Kinnison MT. Human influences on rates of phenotypic change in wild animal populations. Mol Ecol. 2008;17(1):20–9.

3. Hendry AP, Gotanda KM, Svensson EI. Human influences on evolution, and the ecological and societal consequences. Philos Trans R Soc Lond B Biol Sci. 2017;372(1712).

670 4. Palumbi SR. Humans as the World's Greatest Evolutionary Force. Science.
671 2001;293(5536):1786–90.

672 5. Ffrench-Constant RH, Daborn PJ, Le Goff G. The genetics and genomics of insecticide resistance.
673 Trends Genet. 2004;20(3):163–70.

674 6. Liu. Insecticide Resistance in Mosquitoes: Impact, Mechanisms, and Research Directions. Annu
675 Rev Entomol. 2015;60(1):537–59.

676 7. Bass C, Jones CM. Editorial overview: Pests and resistance: Resistance to pesticides in arthropod
677 crop pests and disease vectors: mechanisms, models and tools. Curr Opin Insect Sci.
678 2018;27:iv–vii.

679 8. Dusfour I, Vontas J, David JP, Weetman D, Fonseca DM, Corbel V, et al. Management of
680 insecticide resistance in the major Aedes vectors of arboviruses: Advances and challenges. PLoS
681 Negl Trop Dis. 2019;13(10):e0007615.

682 9. Hawkins NJ, Bass C, Dixon A, Neve P. The evolutionary origins of pesticide resistance. Biol Rev
683 Camb Philos Soc. 2018;94(1):135-155.

684 10. Li XC, Schuler MA, Berenbaum MR. Molecular mechanisms of metabolic resistance to synthetic
685 and natural xenobiotics. Annu Rev Entomol. 2007;52:231–53.

686 11. Brown JE, Evans BR, Zheng W, Obas V, Barrera-Martinez L, Egizi A, et al. Human impacts have
687 shaped historical and recent evolution in *Aedes aegypti*, the dengue and yellow fever mosquito.
688 Evolution. 2014;68(2):514–25.

689 12. Paupy C, Delatte H, Bagny L, Corbel V, Fontenille D. Aedes albopictus, an arbovirus vector: from
690 the darkness to the light. Microbes Infect Inst Pasteur. 2009;11(14–15):1177–85.

691 13. Bonizzoni M, Gasperi G, Chen X, James AA. The invasive mosquito species Aedes albopictus:
692 current knowledge and future perspectives. Trends Parasitol. 2013;29(9):460–8.

693 14. Carvalho VL, Long MT. Perspectives on New Vaccines against Arboviruses Using Insect-Specific
694 Viruses as Platforms. Vaccines. 2021;9(3):263.

695 15. Garg H, Mehmetoglu-Gurbuz T, Joshi A. Virus Like Particles (VLP) as multivalent vaccine
696 candidate against Chikungunya, Japanese Encephalitis, Yellow Fever and Zika Virus. Sci Rep.
697 2020;10(1):4017.

698 16. Silva JVJ, Lopes TRR, Oliveira-Filho EFD, Oliveira RAS, Durães-Carvalho R, Gil LHVG. Current status,
699 challenges and perspectives in the development of vaccines against yellow fever, dengue, Zika
700 and chikungunya viruses. Acta Trop. 2018;182:257–63.

701 17. Moyes CL, Vontas J, Martins AJ, Ng LC, Koou SY, Dusfour I, et al. Contemporary status of
702 insecticide resistance in the major Aedes vectors of arboviruses infecting humans. PLoS Negl Trop
703 Dis. 2017;11(7):e0005625.

704 18. Van Den Berg H, Da Silva Bezerra HS, Al-Eryani S, Chanda E, Nagpal BN, Knox TB, et al. Recent
705 trends in global insecticide use for disease vector control and potential implications for
706 resistance management. Sci Rep. 2021;11(1):23867.

707 19. Dusfour I, Thalmensy V, Gaborit P, Issaly J, Carinci R, Girod R. Multiple insecticide resistance in
708 *Aedes aegypti* (Diptera: Culicidae) populations compromises the effectiveness of dengue vector
709 control in French Guiana. Mem Inst Oswaldo Cruz. 2011;106(3):346–52.

710 20. Marcombe S, Carron A, Darriet F, Etienne M, Agnew P, Tolosa M, et al. Reduced efficacy of
711 pyrethroid space sprays for dengue control in an area of Martinique with pyrethroid resistance.
712 Am J Trop Med Hyg. 2009;80(5):745–51.

713 21. Marcombe S, Darriet F, Tolosa M, Agnew P, Duchon S, Etienne M, et al. Pyrethroid resistance
714 reduces the efficacy of space sprays for dengue control on the island of Martinique (Caribbean).
715 PLoS Negl Trop Dis. 2011;5(6):e1202.

716 22. Valle D, Bellinato DF, Viana-Medeiros PF, Lima JBP, Martins Junior ADJ. Resistance to temephos
717 and deltamethrin in Aedes aegypti from Brazil between 1985 and 2017. Mem Inst Oswaldo Cruz.
718 2019;114:e180544.

719 23. Smith LB, Kasai S, Scott JG. Pyrethroid resistance in *Aedes aegypti* and *Aedes albopictus*:
720 Important mosquito vectors of human diseases. Pestic Biochem Physiol. 2016;133:1–12.

721 24. Soderlund DM. Molecular mechanisms of pyrethroid insecticide neurotoxicity: recent advances.
722 Arch Toxicol. 2012;86(2):165–81.

723 25. Auteri M, La Russa F, Blanda V, Torina A. Insecticide Resistance Associated with *kdr* Mutations in
724 *Aedes albopictus*: An Update on Worldwide Evidences. BioMed Res Int. 2018;2018:1–10.

725 26. Endersby-Harshman NM, Schmidt TL, Hoffmann AA. Diversity and distribution of sodium channel
726 mutations in *Aedes albopictus* (Diptera: Culicidae). Healy K, éditeur. J Med Entomol.
727 2024;61(3):630–43.

728 27. Soderlund DM, Knipple DC. The molecular biology of knockdown resistance to pyrethroid
729 insecticides. Insect Biochem Mol Biol. 2003;33(6):563–77.

730 28. Uemura N, Itokawa K, Komagata O, Kasai S. Recent advances in the study of knockdown
731 resistance (kdr) mutations in Aedes mosquitoes with a focus on several remarkable mutations.
732 Curr Opin Insect Sci. 2024;101178.

733 29. Chambers J. An introduction to the metabolism of pyrethroids. In: Gunther FA, Gunther JD,
734 éditeurs. Residue Reviews [Internet]. New York, NY: Springer New York; 1980. p. 101–24.
735 (Reviews of Environmental Contamination and Toxicology; vol. 73).
736 http://link.springer.com/10.1007/978-1-4612-6068-4_7

737 30. Dermauw W, Van Leeuwen T. The ABC gene family in arthropods: Comparative genomics and
738 role in insecticide transport and resistance. Insect Biochem Mol Biol. 2014;45:89–110.

739 31. Panini M, Manicardi GC, Moores GD, Mazzoni E. An overview of the main pathways of metabolic
740 resistance in insects. Invertebr Surviv J. 2016;326-335 Pages.

741 32. Faucon F, Dusfour I, Gaude T, Navratil V, Boyer F, Chandre F, et al. Identifying genomic changes
742 associated with insecticide resistance in the dengue mosquito Aedes aegypti by deep targeted
743 sequencing. Genome Res. 2015;25(9):1347–59.

744 33. Ffrench-Constant RH. The molecular genetics of insecticide resistance. Genetics.
745 2013;194(4):807–15.

746 34. Lucas ER, Miles A, Harding NJ, Clarkson CS, Lawniczak MK, Kwiatkowski DP, et al. Whole genome
747 sequencing reveals high complexity of copy number variation at insecticide resistance loci in
748 malaria mosquitoes. BioRxiv. 2018;http://dx.doi.org/10.1101/39956.

749 35. Weetman D, Djogbenou LS, Lucas E. Copy number variation (CNV) and insecticide resistance in
750 mosquitoes: evolving knowledge or an evolving problem? Curr Opin Insect Sci. 2018;27:82–8.

751 36. Chuaycharoensuk T, Juntarajumnong W, Boonyuan W, Bangs MJ, Akratanakul P, Thammapalo S,
752 et al. Frequency of pyrethroid resistance in Aedes aegypti and Aedes albopictus (Diptera:
753 Culicidae) in Thailand. J Vector Ecol. 2011;36(1):204–12.

754 37. Ishak HI, Zairi J, Ranson H, Wondji C. Contrasting patterns of insecticide resistance and
755 knockdown resistance (kdr) in the dengue vectors *Aedes aegypti* and *Aedes albopictus* from
756 Malaysia. Parasit Vectors. 2015;8:181.

757 38. Lee RML, Choong CTH, Goh BPL, Ng LC, Lam-Phua SG. Bioassay and biochemical studies of the
758 status of pirimiphos-methyl and cypermethrin resistance in Aedes (Stegomyia) aegypti and Aedes
759 (Stegomyia) albopictus (Diptera: Culicidae) in Singapore. Trop Biomed. 2014;31(4):670–9.

760 39. Thanispong K, Sathantriphop S, Malaithong N, Bangs MJ, Chareonviriyaphap T. Establishment of
761 Diagnostic Doses of Five Pyrethroids for Monitoring Physiological Resistance in Aedes Albopictus
762 in Thailand. J Am Mosq Control Assoc. 2015;31(4):346–52.

763 40. Gao JP, Chen HM, Shi H, Peng H, Ma YJ. Correlation between adult pyrethroid resistance and
764 knockdown resistance (kdr) mutations in Aedes albopictus (Diptera: Culicidae) field populations
765 in China. Infect Dis Poverty. 2018;7(1):86.

766 41. Kushwah RBS, Mallick PK, Ravikumar H, Dev V, Kapoor N, Adak TP, et al. Status of DDT and
767 pyrethroid resistance in Indian Aedes albopictus and absence of knockdown resistance (kdr)
768 mutation. J Vector Borne Dis. 2015;52(1):95–8.

769 42. Mohsin M, Naz S, Khan I, Jabeen A, Bilal H, Ahmed R, et al. Susceptibility status of Aedes aegypti
770 and Aedes albopictus against insecticides at eastern Punjab, Pakistan. Int J Mosq Res.
771 2016;3:41–6.

772 43. Kasai S, Caputo B, Tsunoda T, Cuong TC, Maekawa Y, Lam-Phua SG, et al. First detection of a Vssc
773 allele V1016G conferring a high level of insecticide resistance in Aedes albopictus collected from
774 Europe (Italy) and Asia (Vietnam), 2016: a new emerging threat to controlling arboviral diseases.
775 Euro Surveill Bull Eur Sur Mal Transm Eur Commun Dis Bull. 2019;24(5).

776 44. Zhou X, Yang C, Liu N, Li M, Tong Y, Zeng X, et al. Knockdown resistance (kdr) mutations within
777 seventeen field populations of Aedes albopictus from Beijing China: first report of a novel
778 V1016G mutation and evolutionary origins of kdr haplotypes. Parasit Vectors. 2019;12(1):180.

779 45. Ishak IH, Riveron JM, Ibrahim SS, Stott R, Longbottom J, Irving H, et al. The Cytochrome P450
780 gene CYP6P12 confers pyrethroid resistance in kdr-free Malaysian populations of the dengue
781 vector *Aedes albopictus*. Sci Rep. 2016;6:24707.

782 46. Marcombe S, Doeurk B, Thammavong P, Veseli T, Heafield C, Mills MA, et al. Metabolic
783 Resistance and Not Voltage-Gated Sodium Channel Gene Mutation Is Associated with Pyrethroid
784 Resistance of Aedes albopictus (Skuse, 1894) from Cambodia. Insects. 2024;15(5):358.

785 47. Xu J, Su X, Bonizzoni M, Zhong D, Li Y, Zhou G, et al. Comparative transcriptome analysis and RNA
786 interference reveal CYP6A8 and SNPs related to pyrethroid resistance in Aedes albopictus.
787 Attardo GM, éditeur. PLoS Negl Trop Dis. 2018;12(11):e0006828.

788 48. Pichler V, Bellini R, Veronesi R, Arnoldi D, Rizzoli A, Lia RP, et al. First evidence of resistance to
789 pyrethroid insecticides in Italian *AEDES ALBOPICTUS* populations 26 years after invasion. Pest
790 Manag Sci. 2018;74(6):1319–27.

791 49. Pichler V, Malandruccolo C, Paola S, Bellini R, Severini F, Toma L, et al. Phenotypic and genotypic
792 pyrethroid resistance of Aedes albopictus, with focus on the 2017 chikungunya outbreak in Italy.
793 Pest Manag Sci. 2019;

794 50. Pichler V, Caputo B, Valadas V, Micocci M, Horvath C, Virgillito C, et al. Geographic distribution of
795 the V1016G knockdown resistance mutation in Aedes albopictus: a warning bell for Europe.
796 Parasit Vectors. 2022;15(1):280.

797 51. Djiappi-Tchamen B, Nana-Ndjangwo MS, Mavridis K, Talipouo A, Nchoutpouen E, Makoudjou I, et
798 al. Analyses of Insecticide Resistance Genes in Aedes aegypti and Aedes albopictus Mosquito
799 Populations from Cameroon. Genes. 2021;12(6):828.

800 52. Yamashita S, Uruma K, Yang C, Higa Y, Minakawa N, Cuamba N, et al. The origin and insecticide
801 resistance of Aedes albopictus mosquitoes established in southern Mozambique. Parasit Vectors.
802 2024;17(1):292.

803 53. Yougang AP, Keumeni CR, Wilson-Bahun TA, Tedjou AN, Njiokou F, Wondji C, et al. Spatial
804 distribution and insecticide resistance profile of Aedes aegypti and Aedes albopictus in Douala,
805 the most important city of Cameroon. Plos One. 2022;17(12):e0278779.

806 54. Delatte H, Dehecq JS, Thiria J, Domerg C, Paupy C, Fontenille D. Geographic Distribution and
807 Developmental Sites of *Aedes albopictus* (Diptera: Culicidae) During a Chikungunya Epidemic
808 Event. Vector-Borne Zoonotic Dis. 2008;8(1):25–34.

809 55. Delatte H, Paupy C, Dehecq JS, Thiria J, Failloux AB, Fontenille D. *Aedes albopictus* , vecteur des
810 virus du chikungunya et de la dengue à la Réunion: biologie et contrôle. Parasite.
811 2008;15(1):3–13.

812 56. Renault P, Solet JL, Sissoko D, Balleydier E, Larrieu S, Filleul L, et al. A major epidemic of
813 chikungunya virus infection on Reunion Island, France, 2005-2006. Am J Trop Med Hyg.
814 2007;77(4):727–31.

815 57. Vincent M, Paty MC, Gerardin P, Balleydier E, Etienne A, Daoudi J, et al. From dengue outbreaks
816 to endemicity: Reunion Island, France, 2018 to 2021. Eurosurveillance. 2023;28(29).

817 58. Expertise from the French National Agency for Health, Food and Environmental Safety (ANSES)
818 n°2020-SA-0029. Résistance des moustiques vecteurs aux insecticides. 2020.
819 https://www.anses.fr/fr/system/files/BIOCIDES2020SA0029Ra.pdf

820 59. Tancredi A, Papandrea D, Marconcini M, Carballar-Lejarazu R, Casas-Martinez M, Lo E, et al.
821 Tracing temporal and geographic distribution of resistance to pyrethroids in the arboviral vector
822 Aedes albopictus. Aldridge RL, éditeur. PLoS Negl Trop Dis. 2020;14(6):e0008350.

823 60. Chandor-Proust A, Bibby J, Regent-Kloeckner M, Roux J, Guittard-Crilat E, Poupardin R, et al. The
824 central role of mosquito cytochrome P450 CYP6Zs in insecticide detoxification revealed by
825 functional expression and structural modelling. Biochem J. 2013;455:75–85.

826 61. Nikou D, Ranson H, Hemingway J. An adult-specific CYP6P450 gene is overexpressed in a
827 pyrethroid-resistant strain of the malaria vector, Anopheles gambiae. Gene. 2003;318:91–102.

828 62. Vontas J, Katsavou E, Mavridis K. Cytochrome P450-based metabolic insecticide resistance in
829 Anopheles and Aedes mosquito vectors: Muddying the waters. Pestic Biochem Physiol.
830 2020;170:104666.

831 63. Stevenson BJ, Bibby J, Pignatelli P, Muangnoicharoen S, O'Neill PM, Lian LY, et al. Cytochrome
832 P450 6M2 from the malaria vector *Anopheles gambiae* metabolizes pyrethroids: Sequential
833 metabolism of deltamethrin revealed. Insect Biochem Mol Biol. 2011;41(7):492–502.

834 64. Kouamo MFM, Ibrahim SS, Hearn J, Riveron JM, Kusimo M, Tchouakui M, et al. Genome-Wide
835 Transcriptional Analysis and Functional Validation Linked a Cluster of Epsilon Glutathione S-
836 Transferases with Insecticide Resistance in the Major Malaria Vector Anopheles funestus across
837 Africa. Genes. 2021;12(4):561.

838 65. Messenger LA, Impoinvil LM, Derilus D, Yewhalaw D, Irish S, Lenhart A. A whole transcriptomic
839 approach provides novel insights into the molecular basis of organophosphate and pyrethroid
840 resistance in Anopheles arabiensis from Ethiopia. Insect Biochem Mol Biol. 2021;139:103655.

841 66. Simma EA, Dermauw W, Balabanidou V, Snoeck S, Bryon A, Clark RM, et al. Genome-wide gene
842 expression profiling reveals that cuticle alterations and P450 detoxification are associated with
843 deltamethrin and DDT resistance in Anopheles arabiensis populations from Ethiopia. Pest Manag
844 Sci. 2019;75(7):1808–18.

845 67. Tao F, Si F, Hong R, He X, Li X, Qiao L, et al. Glutathione *S* -transferase (GST) genes and their
846 function associated with pyrethroid resistance in the malaria vector *Anopheles sinensis*. Pest
847 Manag Sci. 2022;78(10):4127–39.

848 68. Bariami V, Jones CM, Poupardin R, Vontas J, Ranson H. Gene Amplification, ABC Transporters and
849 Cytochrome P450s: Unraveling the Molecular Basis of Pyrethroid Resistance in the Dengue
850 Vector, Aedes aegypti. PLoS Negl Trop Dis. 2012;6(6).

851 69. Bonizzoni M, Afrane Y, Dunn WA, Atieli FK, Zhou G, Zhong D, et al. Comparative transcriptome
852 analyses of deltamethrin-resistant and -susceptible Anopheles gambiae mosquitoes from Kenya
853 by RNA-Seq. PloS One. 2012;7(9):e44607.

854 70. Epis S, Porretta D, Mastrantonio V, Urbanelli S, Sassera D, De Marco L, et al. Temporal dynamics
855 of the ABC transporter response to insecticide treatment: insights from the malaria vector
856 Anopheles stephensi. Sci Rep. 2014;4(1):7435.

857 71. He Q, Yan Z, Si F, Zhou Y, Fu W, Chen B. ATP-Binding Cassette (ABC) Transporter Genes Involved
858 in Pyrethroid Resistance in the Malaria Vector Anopheles sinensis: Genome-Wide Identification,
859 Characteristics, Phylogenetics, and Expression Profile. Int J Mol Sci. 2019;20(6):1409.

860 72. Mastrantonio V, Ferrari M, Epis S, Negri A, Scuccimarra G, Montagna M, et al. Gene expression
861 modulation of ABC transporter genes in response to permethrin in adults of the mosquito
862 malaria vector Anopheles stephensi. Acta Trop. 2017;171:37–43.

863 73. Xu J, Zheng J, Zhang R, Wang H, Du J, Li J, et al. Identification and functional analysis of ABC
864 transporter genes related to deltamethrin resistance in *Culex pipiens pallens*. Pest Manag Sci.
865 2023;79(10):3642–55.

866 74. Scheuer T. Regulation of sodium channel activity by phosphorylation. Semin Cell Dev Biol.
867 2011;22(2):160–5.

868 75. Srinivasan Y, Elmer L, Davis J, Bennett V, Angelides K. Ankyrin and spectrin associate with voltage-
869 dependent sodium channels in brain. Nature. 1988;333(6169):177–80.

870 76. Manni M, Guglielmino CR, Scolari F, Vega-Rua A, Failloux AB, Somboon P, et al. Genetic evidence
871 for a worldwide chaotic dispersion pattern of the arbovirus vector, Aedes albopictus. PLoS Negl
872 Trop Dis. 2017;11(1):e0005332.

873 77. Maynard AJ, Ambrose L, Cooper RD, Chow WK, Davis JB, Muzari MO, et al. Tiger on the prowl:
874 Invasion history and spatio-temporal genetic structure of the Asian tiger mosquito Aedes
875 albopictus (Skuse 1894) in the Indo-Pacific. Vasilakis N, éditeur. PLoS Negl Trop Dis.
876 2017;11(4):e0005546.

877 78. Mousson L, Dauga C, Garrigues T, Schaffner F, Vazeille M, Failloux AB. Phylogeography of *Aedes* (
878 *Stegomyia*) *aegypti* (L.) and *Aedes* (*Stegomyia*) *albopictus* (Skuse) (Diptera: Culicidae) based on
879 mitochondrial DNA variations. Genet Res. 2005;86(1):1–11.

880 79. Chen H, Li K, Wang X, Yang X, Lin Y, Cai F, et al. First identification of kdr allele F1534S in VGSC
881 gene and its association with resistance to pyrethroid insecticides in Aedes albopictus
882 populations from Haikou City, Hainan Island, China. Infect Poverty. 2016;5:31.

883 80. David JP, Ismail HM, Chandor-Proust A, Paine MJ. Role of cytochrome P450s in insecticide
884 resistance: impact on the control of mosquito-borne diseases and use of insecticides on Earth.
885 Philos Trans R Soc Lond B Biol Sci. 2013;368(1612):20120429.

886 81. Bengoa M, Eritja R, Delacour S, Miranda MA, Sureda A, Lucientes J. First Data on Resistance to
887 Pyrethroids in Wild Populations of Aedes albopictus from Spain. J Am Mosq Control Assoc.
888 2017;33(3):246–9.

889 82. Chen HM. Role of metabolic detoxification enzyme activity and knockdown resistance gene
890 mutations in resistance of aedes albopictus to pyrethroid insecticides. Acad J Second Mil Med
891 Univ. 2019;512–9.

892 83. Khan HAA. Resistance to insecticides and synergism by enzyme inhibitors in Aedes albopictus
893 from Punjab, Pakistan. Sci Rep. 2020;10(1):21034.

894 84. Li Y, Xu J, Zhong D, Zhang H, Yang W, Zhou G, et al. Evidence for multiple-insecticide resistance in
895 urban Aedes albopictus populations in southern China. Parasit Vectors. 2018;11(1):4.

896 85. Feyereisen R. Insect P450 enzymes. Annu Rev Entomol. 1999;44:507–33.

897 86. Bacot T, Haberkorn C, Guilliet J, Cattel J, Kefi M, Nadalin L, et al. A genomic duplication spanning
898 multiple P450s contributes to insecticide resistance in the dengue mosquito Aedes aegypti. Peer
899 Community J. 2024;4:e110.

900 87. Cattel J, Haberkorn C, Laporte F, Gaude T, Cumer T, Renaud J, et al. A genomic amplification
901 affecting a carboxylesterase gene cluster confers organophosphate resistance in the mosquito
902 *Aedes aegypti*: From genomic characterization to high-throughput field detection. Evol Appl.
903 2021;14(4):1009–22.

904 88. Remnant EJ, Good RT, Schmidt JM, Lumb C, Robin C, Daborn PJ, et al. Gene duplication in the
905 major insecticide target site, *Rdl* , in *Drosophila melanogaster*. Proc Natl Acad Sci.
906 2013;110(36):14705–10.

907 89. Melo ESD, Wallau GL. Mosquito genomes are frequently invaded by transposable elements
908 through horizontal transfer. Malik HS, éditeur. Plos Genet. 2020;16(11):e1008946.

909 90. Nene V, Wortman JR, Lawson D, Haas B, Kodira C, Tu ZJ, et al. Genome sequence of *Aedes*
910 *aegypti*, a major arbovirus vector. Science. 2007;316(5832):1718–23.

911 91. Palatini U, Masri RA, Cosme LV, Koren S, Thibaud-Nissen F, Biedler JK, et al. Improved reference
912 genome of the arboviral vector Aedes albopictus. Genome Biol. 2020;21(1):215.

913 92. Amezian D, Nauen R, Le Goff G. Transcriptional regulation of xenobiotic detoxification genes in
914 insects - An overview. Pestic Biochem Physiol. 2021;174:104822.

915 93. Ji M, Vandenhole M, De Beer B, De Rouck S, Villacis-Perez E, Feyereisen R, et al. A nuclear
916 receptor HR96-related gene underlies large trans-driven differences in detoxification gene
917 expression in a generalist herbivore. Nat Commun. 2023;14(1):4990.

918 94. Wen X, Feng K, Qin J, Wei P, Cao P, Zhang Y, et al. A detoxification pathway initiated by a nuclear
919 receptor TcHR96h in Tetranychus cinnabarinus (Boisduval). Palli SR, éditeur. Plos Genet.
920 2023;19(9):e1010911.

921 95. Lien NTK, Ngoc NTH, Lan NN, Hien NT, Tung NV, Ngan NTT, et al. Transcriptome Sequencing and
922 Analysis of Changes Associated with Insecticide Resistance in the Dengue Mosquito (Aedes
923 aegypti) in Vietnam. Am J Trop Med Hyg. 2019;100(5):1240–8.

924 96. Shan G, Hammock BD. Development of Sensitive Esterase Assays Based on α-Cyano-Containing
925 Esters. Anal Biochem. 2001;299(1):54–62.

926 97. Faria R, Johannesson K, Butlin RK, Westram AM. Evolving Inversions. Trends Ecol Evol.
927 2019;34(3):239–48.

928 98. Haberkorn C, David J, Henri H, Delpuech J, Lasseur R, Vavre F, et al. A major 6 Mb superlocus is
929 involved in pyrethroid resistance in the common bed bug *Cimex lectularius*. Evol Appl.
930 2023;16(5):1012–28.

931 99. Wellenreuther M, Mérot C, Berdan E, Bernatchez L. Going beyond SNPs: The role of structural
932 genomic variants in adaptive evolution and species diversification. Mol Ecol. 2019;28(6):1203–9.

933 100. Wellenreuther M, Bernatchez L. Eco-Evolutionary Genomics of Chromosomal Inversions. Trends
934 Ecol Evol. 2018;33(6):427–40.

935 101. Deng J, Guo Y, Su X, Liu S, Yang W, Wu Y, et al. Impact of deltamethrin-resistance in Aedes
936 albopictus on its fitness cost and vector competence. Churcher TS, éditeur. PLoS Negl Trop Dis.
937 2021;15(4):e0009391.

938 102. Standard operating procedure for testing insecticide susceptibility of adult mosquitoes in WHO
939 tube tests. SOP version: WHO Tube test/01/14. World Health Organization; 2022.
940 https://iris.who.int/bitstream/handle/10665/352316/9789240043831-eng.pdf?sequence=1

941 103. Boyle JH, Rastas PMA, Huang X, Garner AG, Vythilingam I, Armbruster PA. A Linkage-Based
942 Genome Assembly for the Mosquito Aedes albopictus and Identification of Chromosomal
943 Regions Affecting Diapause. Insects. 2021;12(2):167.

944 104. Chen Y, Chen Y, Shi C, Huang Z, Zhang Y, Li S, et al. SOAPnuke: a MapReduce acceleration-
945 supported software for integrated quality control and preprocessing of high-throughput
946 sequencing data. GigaScience. 2018;7(1):1-6.

947 105. Andrews S. FastQC: a quality control tool for high throughput sequence data. 2010. Available
948 online at: http://www.bioinformatics.babraham.ac.uk/projects/fastqc/

949 106. Dobin A, Davis CA, Schlesinger F, Drenkow J, Zaleski C, Jha S, et al. STAR: ultrafast universal RNA-
950 seq aligner. Bioinformatics. 2013;29(1):15–21.

951 107. Benjamini Y, Hochberg Y. Controlling the False Discovery Rate: a Practical and Powerful Approach
952 to Multiple Testing. J R Stat Soc B. 1995;57:289–300.

953 108. Giraldo-Calderón GI, Harb OS, Kelly SA, Rund SS, Roos DS, McDowell MA. VectorBase.org
954 updates: bioinformatic resources for invertebrate vectors of human pathogens and related
955 organisms. Curr Opin Insect Sci. 2022;50:100860.

956 109. Harb OS, McDowell MA, Roos DS. VEuPathDB Resources: A Platform for Free Online Data
957 Exploration, Integration, and Analysis. In: Setubal JC, Stadler PF, Stoye J, editors. Comparative
958 Genomics. New York, NY: Springer US; 2024 p. 573–86. (Methods in Molecular Biology; vol.
959 2802).

960 110. Lemoine F, Correia D, Lefort V, Doppelt-Azeroual O, Mareuil F, Cohen-Boulakia S, et al.
961 NGPhylogeny.fr: new generation phylogenetic services for non-specialists. Nucleic Acids Res.
962 2019;47(W1):W260–5.

963 111. Sacomoto GA, Kielbassa J, Chikhi R, Uricaru R, Antoniou P, Sagot MF, et al. KIS SPLICE: de-novo
964 calling alternative splicing events from RNA-seq data. BMC Bioinformatics. 2012;13(S6):S5.

965 112. Benoit-Pilven C, Marchet C, Chautard E, Lima L, Lambert MP, Sacomoto G, et al. Complementarity
966 of assembly-first and mapping-first approaches for alternative splicing annotation and
967 differential analysis from RNAseq data. Sci Rep. 2018;8(1):4307.

968 113. Li H, Durbin R. Fast and accurate short read alignment with Burrows-Wheeler transform.
969 Bioinformatics. 2009;25(14):1754–60.

970 114. Li H, Handsaker B, Wysoker A, Fennell T, Ruan J, Homer N, et al. The Sequence Alignment/Map
971 format and SAMtools. Bioinforma Oxf Engl. 2009;25(16):2078–9.

972 115. Schrider DR, BEGUN DJ, HAHN MW. Detecting highly differentiated copy-number variants from
973 pooled population sequencing. Pac Symp Biocomput Pac Symp Biocomput. 2013;344–55.

974 116. Danecek P, Bonfield JK, Liddle J, Marshall J, Ohan V, Pollard MO, et al. Twelve years of SAMtools
975 and BCFtools. Gigascience. 2021;10(2):giab008.

976 117. Cingolani P, Platts A, Wang LL, Coon M, Nguyen T, Wang L, et al. A program for annotating and
977 predicting the effects of single nucleotide polymorphisms, SnpEff: SNPs in the genome of
978 Drosophila melanogaster strain w^{1118}; iso-2; iso-3. Fly. 2012;6(2):80–92.

979 118. Lin L qun, Chen Y hui, Tian Y fan, Chen Y sen, Zheng Z yang, Wu J xin, et al. Study on the cross-
980 resistance of Aedes albopictus (Skuse) (Diptera: Culicidae) to deltamethrin and pyriproxyfen.
981 Parasit Vectors. 2024;17(1):403.